BILINGUAL PUBLISHING GROUP

Journal of Environmental & Earth Sciences

https://journals.bilpubgroup.com/index.php/jees

ARTICLE

Development of a Two-Dimensional Hydrodynamic Model to Simulate Rip Currents in the Bai Dai-Cam Ranh Coast, Vietnam

Ngo Nam Thinh [1,2,3] **, *Nguyen Thi Bay*** [4*]

[1] *Department of Oceanology, Meteorology and Hydrology, Faculty of Physics-Engineering Physics, University of Science, Ho Chi Minh City 700000, Vietnam*

[2] *Viet Nam National University-Ho Chi Minh, Ho Chi Minh City 700000, Vietnam*

[3] *Faculty of Environment, Ho Chi Minh City University of Natural Resources and Environment, Ho Chi Minh City 700000, Vietnam*

[4] *Institute of Applied Technology and Sustainable Development, Nguyen Tat Thanh University, Ho Chi Minh City 700000, Vietnam*

ABSTRACT

Rip currents are a significant threat to swimmers worldwide, responsible for numerous drowning incidents each year. In Vietnam, Bai Dai Beach in Cam Ranh Bay, Khanh Hoa Province, has experienced an increase in drowning events due to rip currents in recent years. To address this issue, a comprehensive study was conducted based on developing a depth-averaged 2D hydrodynamic model to simulate rip currents in the Bai Dai-Cam Ranh coast. The HYDIST-2D numerical model was applied to simulate the rip current evolution in space and time for the study area. The results showed that the HYDIST-2D numerical model can accurately predict the location, magnitude, and microstructure of rip currents, including rip current speed, width, and length. The simulation results revealed that the rip current speed is greater during the low tide phase, with an average speed of 0.5 m s^{-1}, while during high tide, the rip current speed is lower, around 0.1–0.8 m s^{-1}. The width and length of the rip current also vary with the tide phase, with a wider and longer rip current observed during the low tide phase. The results also showed that the rip current speed and microstructure are influenced by

*CORRESPONDING AUTHOR:

Nguyen Thi Bay, Institute of Applied Technology and Sustainable Development, Nguyen Tat Thanh University, Ho Chi Minh City 700000, Vietnam; Email: nguyentbay@gmail.com

ARTICLE INFO

Received: 27 January 2025 | Revised: 13 February 2025 | Accepted: 14 February 2025 | Published Online: 31 March 2025
DOI: https://doi.org/10.30564/jees.v7i4.8574

CITATION

Thinh, N.N., Bay, N.T., 2025. Development of a Two-Dimensional Hydrodynamic Model to Simulate Rip Currents in the Bai Dai-Cam Ranh Coast, Vietnam. Journal of Environmental & Earth Sciences. 7(4): 203–216. DOI: https://doi.org/10.30564/jees.v7i4.8574

the wave features, tide current, and bathymetry of the study area. The present study provides valuable insights into the dynamics of rip currents in the Bai Dai-Cam Ranh coast. The findings can be used to support the management of bathing activities and provide early warnings for potential risks associated with rip currents.

Keywords: HYDIST Model; Swimmers; Rip; Hydrodynamic Factors; Breaking Waves

1. Introduction

Rip currents are considered a natural phenomenon that occurs when waves break[1, 2], creating an increase in water depth and driving water towards the sea[3–5]. The formation of rip currents is influenced by various factors, including bathymetry[6, 7], wave height and direction, tide, and beach and bathymetry shape[8, 9]. Rip currents form as water tends to flow alongshore from regions of high waves to regions of lower waves where currents converge to form a seaward flowing rip[7, 9]. According to when waves break, they form an increase in water depth. The water depth can change along a shoreline depending on the height of breaking waves[4, 9]. Rip currents can also be influenced by the presence of bathymetric features, such as sand bars or reefs[10, 11]. In addition, rip currents are frequently found at a sand bar or reef, or a hard structure such as a rocky outcrop, jetty, or pier[11, 12]. These bathymetric features result in variations in wave breaking and setup leading to channelized rip currents[13, 14]. Rip currents are a significant threat to swimmers along swimming beaches worldwide, responsible for numerous drownings each year[12, 13]. The current speed of seaward rip currents has been recorded at 0.8 m s^{-1} [14] and even up to 2.0 m s^{-1} [15]. Globally, there are more than thousands of drownings each year due to rip currents[12, 16, 17]. A study conducted by the United States Lifesaving Association (USLA) reports that more than 80% of the 37,000 beach rescues each year are due to rip currents[13, 18–20]. There has been an increase in the number of associated drowning fatalities in recent years[12, 21]. These strong and narrow channels of fast-moving water flow towards the sea from swimming beaches[15, 16], often forming in swimming beaches with varying wave energy dissipation and water depth[17, 18]. In recent decades, related studies have strongly enhanced the understanding of the dynamics of rip currents[15, 17, 19, 22]. Recognized as one of the major causes of drowning among swimmers around the world, many studies on rip currents have been carried out from laboratory experiments such as reproducing laboratory-scale rip currents on a barred beach by Fang et al.[10]; experimental investigation of bed morphology in the lee of porous submerged breakwaters by Klonaris et al.[17]; and an experimental study of rip channel flow by Drønen et al.[23]. Field surveys to study rip currents have also been conducted, such as the Southeast Coastal Ocean Observing Regional Association (SECOORA) in partnership with the National Oceanic and Atmospheric Administration (NOAA), which used cameras to observe rip currents from wave breaking and then spot rip currents. Murray, Cartwright and Tomlinson[24, 25] used video-imaging to find the transient rip currents on the Gold Coast open beaches. Recently, hydrodynamic model-based approaches to the study of rip currents have been widely exploited in many regions around the world[26–28]. For instance, Hong et al.[26] conducted a numerical simulation on the rip currents interlaced with multichannel sandbars. Xu et al.[27] applied the fully nonlinear mild-slope equation model to simulate the rip current around multiple submerged breakwaters. Wang et al.[28] simulated the rip currents in arc-shaped coastlines based on the numerical model. In Vietnam, Nguyen, Ngo and Tran[29] used the Mike hydraulic model to simulate the rip currents in the Nha Trang Coast area. A study on the possibility of rip currents appearing around the Quy Nhon swimming beaches in Binh Dinh province was conducted by Nguyen and Dang[30]. A rip current simulation on some swimming beaches in the Quang Nam coastal area was also employed by Cong et al.[31]. Nguyen, Ngo and Tran[29] conducted a study on the current rip evolution in the Nha Trang Coast Zone belonging to Khanh Hoa province and reported that rip currents appear at Khanh Hoa beaches during the Northeast monsoon and during storms and active tropical depressions. Recently, Ngo and Nguyen[15] applied the Mike21 to simulate the rip current around the Cam Ranh Bay belonging to the Khanh Hoa Coastal area of Vietnam.

This study aims to simulate rip currents at the Bai Dai swimming beaches in Cam Ranh Bay, Vietnam, utilizing the HYDIST-2D numerical model. The study's findings are

expected to provide valuable insights into the formation and dynamics of rip currents at the beach, which can inform the management of bathing activities and enable early warnings for potential risks associated with rip currents.

2. Materials and Methods

2.1. HYDIST Model Description

HYDIST is a two-dimensional numerical model developed by Nguyen Thi Bay's research group in 2004 and continually improved to date. This is a two-dimensional hydrodynamic model that can simulate two-dimensional flow, bed load transport, and bed morphology changes, among others. In particular, the HYDIST-RC module was developed to calculate coastal currents (rip currents) under the combined effects of tides, waves, and wind[32, 33]. The HYDIST model consists of four main modules: the hydraulic module (HYDIST-HD), the sediment transport module (HYDIST-ST), the riverbank erosion module (HYDIST-RF), and the bathymetry evolution module (HYDIST-BG). The hydraulic calculation module (HYDIST-HD) was developed to simulate river and coastal flow under the influence of flooding, tides, and wind[32, 33]. In the current study, the module for simulating 2D flow those changes with space and time has been applied to simulate rip currents at Bai Dai. In calculating the location and intensity of rip currents in coastal areas, the wave field is a crucial factor and an indispensable input for the HYDIST-RC model. The input wave field to the HYDIST-RC model is the wave radiation stress. Firstly, the SWAN model will be used to simulate the wave field. Then, the calculated results of the wave field will be applied to calculate the wave characteristics (height, direction, and period), and they will be used as the input wave data for the HYDIST-RC module to calculate the wave radiation stress. The 2D hydrodynamic equations describing the flow have been integrated with depth.

The continuity equation has the following form:

$$\frac{\partial \zeta}{\partial t} + \frac{\partial |(h+\zeta)u|}{\partial x} + \frac{\partial |(h+\zeta)v|}{\partial y} = 0 \quad (1)$$

Where: u and v are the flow velocity components in the *x*- and *y*-directions (m s^{-1}), respectively; h is the average water depth (m) and ζ is the water level fluctuation (m).

The momentum equations in the x and y directions have the following form:

$$\begin{aligned} &\frac{\partial u}{\partial t} + u\frac{\partial u}{\partial x} + v\frac{\partial u}{y} - fv = \\ &-g\frac{\partial \zeta}{\partial x} + \frac{\tau_{Sx,wind} - \tau_{Sx,w}}{\rho(h+\zeta)} \\ &-\frac{\tau_{bx,c} + \tau_{bx,w}}{\rho(h+\zeta)} + A\nabla^2 u \end{aligned} \quad (2)$$

$$\begin{aligned} &\frac{\partial v}{\partial t} + u\frac{\partial v}{\partial x} + v\frac{\partial v}{\partial y} + fu = \\ &-g\frac{\partial \zeta}{\partial y} + \frac{\tau_{Sy,wind} - \tau_{Sy,w}}{\rho(h+\zeta)} \\ &-\frac{\tau_{by,c} + \tau_{by,w}}{\rho(h+\zeta)} + A\nabla^2 v \end{aligned} \quad (3)$$

Where A is the horizontal turbulent viscosity coefficient (m^2 s^{-1}); f = 2 Ω sin ϕ; f is the Coriolis parameter (1 s^{-1}); Ω is the Earth's rotation speed; $\tau_{bx,\,c}$ and $\tau_{by,\,c}$ are bottom stress due to flow (N m^{-2}); $\tau_{bx,\,w}$ and $\tau_{by,\,w}$ are bottom stress due to wave (N m^{-2}); $\tau_{Sx,\,wind}$ and $\tau_{Sy,\,wind}$ are water surface tangential stress due to wind (N m^{-2}); $\tau_{Sx,\,w}$ and $\tau_{Sy,\,w}$ are water surface tangential stress due to wave (N m^{-2}).

Accordingly, the wind exerts stress on the water surface represented by the friction velocity. The wind speed on the sea surface is often represented by the height index measuring the wind speed in meters from the water surface level. The surface stress due to wind τ_{Sx}, τ_{Sy} is determined by the following empirical formula:

$$(\tau_{Sx,wind}, \tau_{Sy,wind}) = \rho_a C_d \sqrt{W_x^2 + W_y^2}\,(W_x, W_y) \quad (4)$$

In which: ρ_a is the density of air above sea level (kg m^{-3}); C_d is the wind friction coefficient; $C_d = (0.75 + 0.067\,|W|).10^{-3}$. W = (Wx, Wy) is the wind speed at 10 m above sea level (m s^{-1}).

The change in water surface level and flow under the influence of waves can be described as the horizontal transport of wave energy (x, y). The speed of this transport is equivalent to the force exerted on the water surface as the wave propagates, and these forces, when acting on a volume of water, can result in a net force that is not zero. At a certain limit, when these forces are not balanced by the pressure force, they will act as a force causing flow. The modeling of the flow changes caused by waves is based on the concept of radiation stress (S_{xx}, S_{xy}, S_{yy}) proposed by Longuet-Higgins and Stewart[34]. The tangential stress on the water surface caused by the waves is calculated using the Equations (5) and (6):

$$\tau_{Sx,w} = \frac{\partial S_{xx}}{\partial x} + \frac{\partial S_{xy}}{\partial y} \quad (5)$$

$$\tau_{Sy,w} = \frac{\partial S_{yy}}{\partial y} + \frac{\partial S_{xy}}{\partial x} \quad (6)$$

Radiation stresses (S_{xx}, S_{yy}, S_{xy}) are a surface force that represents the transport of wave energy across a surface. The first index in the notation of radiation stress indicates the direction of energy transport, and the second index represents the component of the energy being transported, with units of N m^{-1}. The formula for calculating radiation stress is determined by the Equations (7), (8), and (9).

$$S_{xx} = E\left(\left(\frac{kh}{sinh2kh} + \frac{1}{2}\right) cos^2\theta + \frac{kh}{sinh2kh}\right) \quad (7)$$

$$S_{yy} = E\left(\left(\frac{kh}{sinh2kh} + \frac{1}{2}\right) sin^2\theta + \frac{kh}{sinh2kh}\right) \quad (8)$$

$$S_{xy} = S_{yx} = E\left(\left(\frac{kh}{sinh2kh} + \frac{1}{2}\right) sin\theta cos\theta\right) \quad (9)$$

Where: θ is the incident wave angle; E is wave energy (E = 1/8 ρgH2); H is wave height (m), k is wave number; h is the water depth value at the calculated location (m).

The relationship between angular frequency and wave number is defined by Equation (10)

$$\sigma = 2\pi/T \quad (10)$$

In the formula (10), σ is calculated by Equation (11)

$$\sigma^2 = gktanhkh \quad (11)$$

2.2. Input Data Setup for HYDIST Model Simulation

The Bai Dai Beach, a popular destination in Cam Ranh Bay, Vietnam (**Figure 1**), has experienced an increase in drowning events due to rip currents. To address this issue, a comprehensive study is conducted to evaluate the rip current generations at the Bai Dai Beach. Bathymetric data was collected from the Nha Trang Institute of Oceanography in digital form and then used with Surfer 13 software to interpolate the depth values within the study domain (**Figure 1**). A quadrilateral grid with a grid spacing of 2 m × 2 m was interpolated to clearly show the wave and flow regimes in the Bai Dai coastal area and to meet the requirements for simulating the rip current in detail.

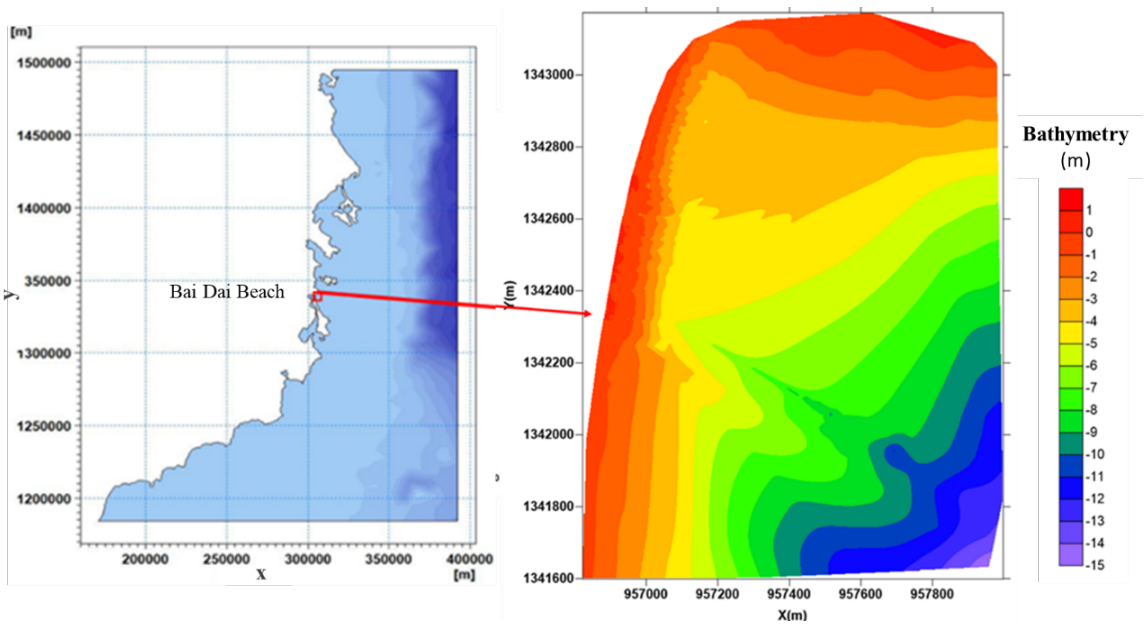

Figure 1. Map of the study area and bathymetric map of Bai Dai Beach Zone.

The water level fluctuation amplitudes were obtained from the global tidal oscillation model with corrections for amplitude and phase of oscillations at the study area as illustrated by **Figure 2**.

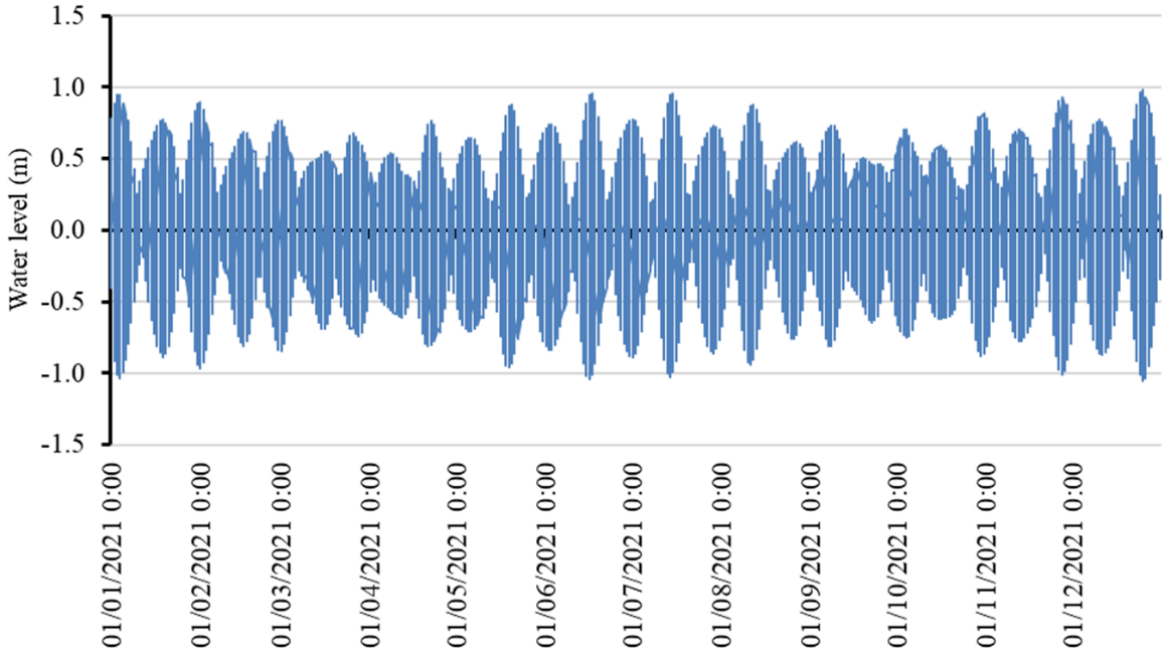

Figure 2. Input water level data for simulating the hydrodynamic processes at Bai Dai Beach Zone.

For the input data for wave height and wave direction simulation, in the large domain, the wave field is calculated from the re-analyzed wind field data of the East Sea area from the global wave prediction model. For the small domain, the input data for wave height and wave direction simulation are the calculation results extracted from the large domain as illustrated in **Figure 3**.

For the input wind data for the simulation model, the spatially and temporally varying wind field was collected from the NOAA reanalysis wind field. The collected wind data was processed and presented as **Figure 4**.

In addition, other main hydrodynamic parameters are set up for the HYDIST model simulation and are presented in **Table 1**.

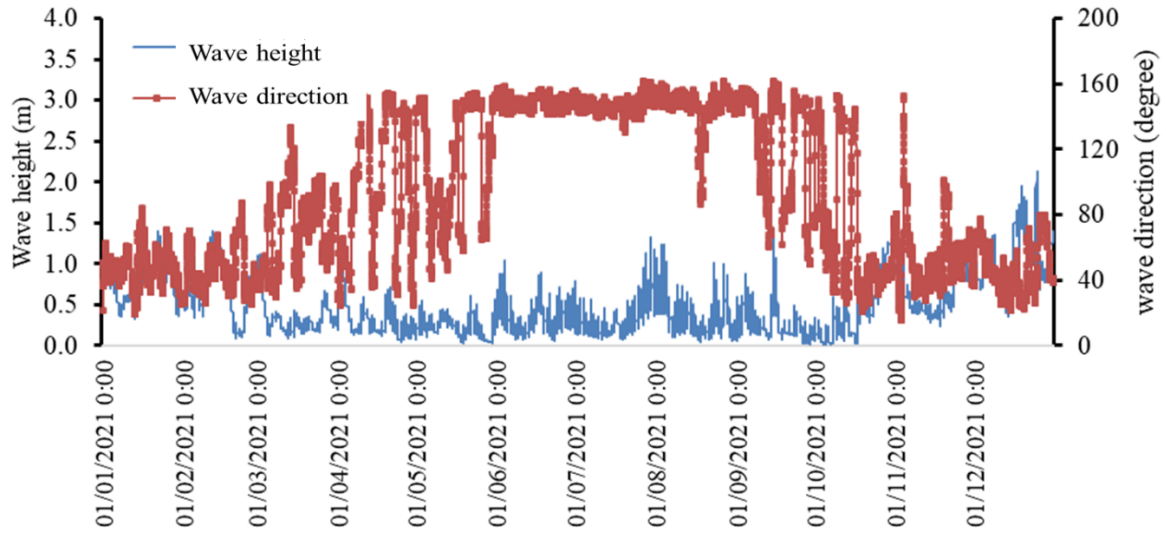

Figure 3. Input wave height and direction for simulating the hydrodynamic processes at the study area.

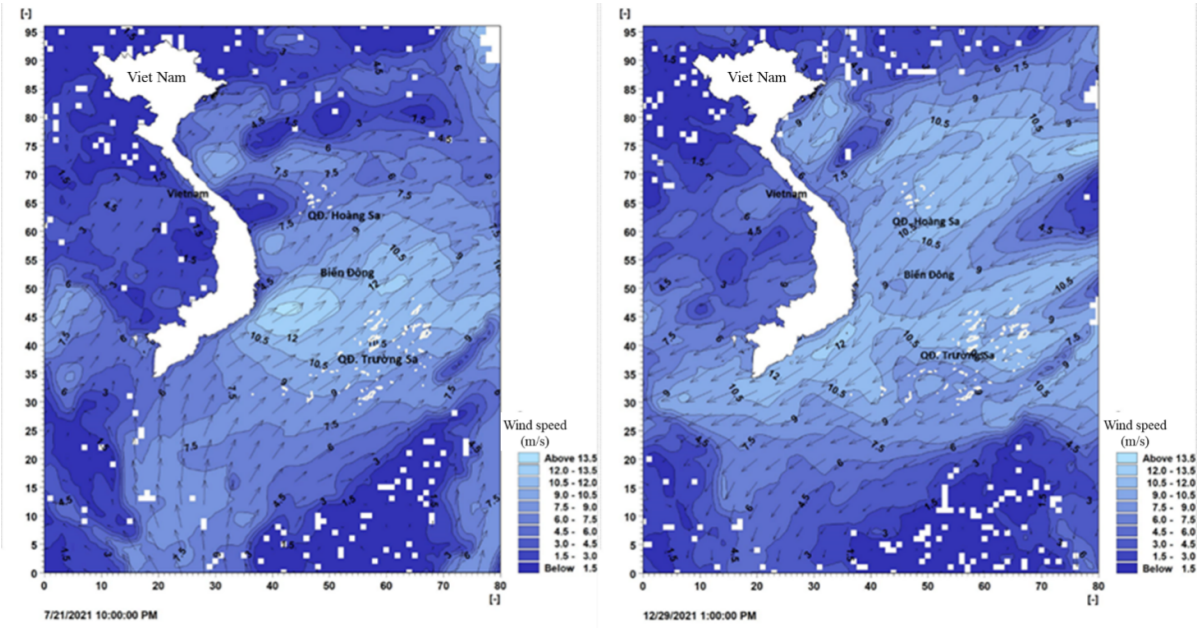

Figure 4. Input wind speed for simulating the hydrodynamic processes at the study area.

Table 1. Summarizing the key input parameters for the HYDIST model simulation.

Parameters	Values	Notes
Δt	0.25 s	Time step for simulating the HYDIST model
T	4.0 hours	Total time of model simulation run
u, v	0	Set initial conditions with no flow
A	0.002 m^2 s^{-1}	Horizontal turbulent viscosity coefficient
n	0.03125	Manning's coefficient
η	0 m	Initial water level

3. Results and Discussion

3.1. Model Calibration and Validation

The HYDIST model performance was calibrated and validated based on the field measurements of waves and currents measured in Ninh Thuan Coast from 23:00 on January 6, 2013, to 9:00 on January 12, 2013, with a time step (Δt) of 1 hour. Through the calibration procedure, the simulation model reaches good results in terms of correlation coefficient (R^2) and NASH index. Specifically, the calibration results in the stage from 23:00 on January 6, 2013, to 9:00 on January 12, 2013 (Northeast monsoon) through the measured and calculated wave height values with the R^2 reaching 0.85 and the NASH up to 0.84 are illustrated in **Figure 5** while the measured and calculated wave period values with an average relative error of 5.28% are shown in **Figure 6**.

For the validation procedure, the simulation model also recorded good results in terms of R^2 and NASH index. Specifically, the validation results in the stage from 11:00 on July 1, 2013, to 11:00 on July 7, 2013 (Southwest monsoon) through the measured and calculated wave height values with the R^2 reaching 0.82 and the NASH = 0.75 are illustrated in **Figure 7** while the measured and calculated wave period values with an average relative error of 5.46% are presented in **Figure 8**.

From the results obtained through calibration and validation procedures, it can be affirmed that the selected model parameters are suitable for applying to simulate rip current evolution in space and time for Bai Dai Beach zone as the research objective has set out.

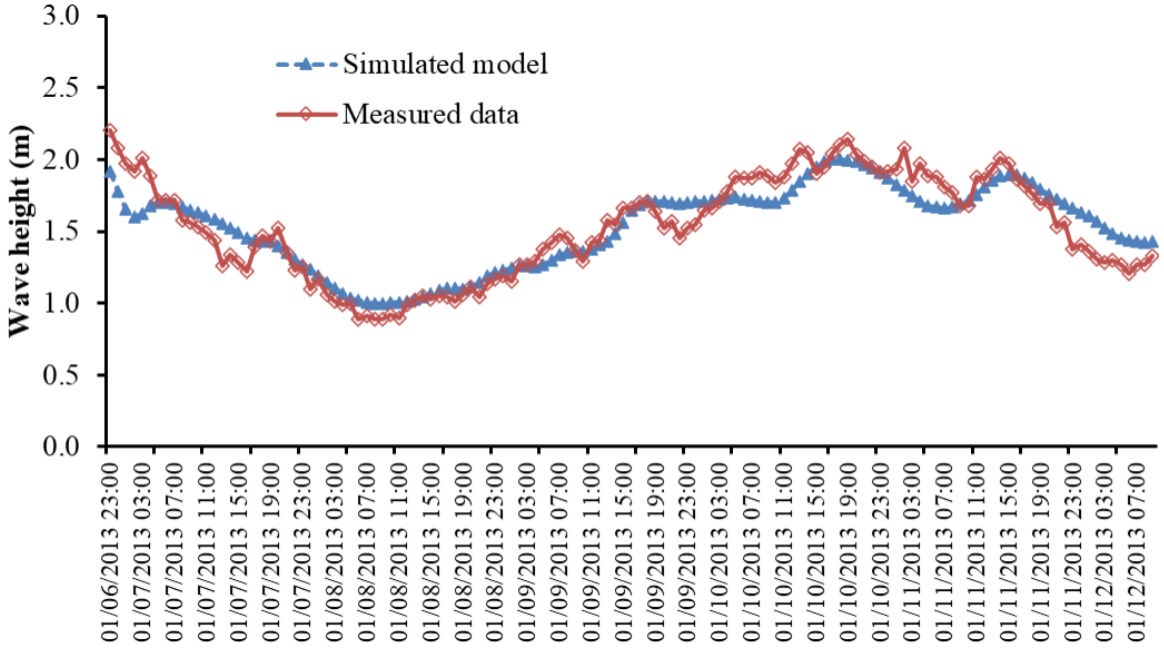

Figure 5. Comparison of the simulated model and measured data wave height during the stage from 06 to 12-Jan-2013 (Northeast monsoon) with $R^2 = 0.85$ and NASH = 0.84.

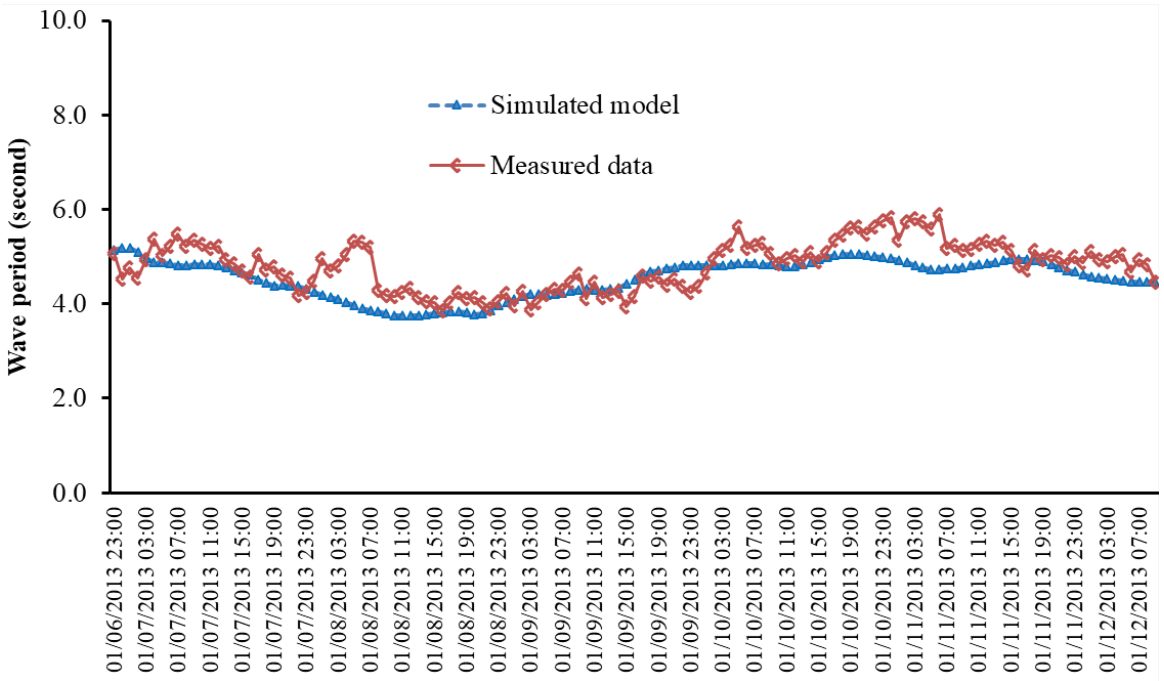

Figure 6. Comparison of the simulated model and measured data wave period during the stage from 06 to 12-Jan-2013(Northeast monsoon).

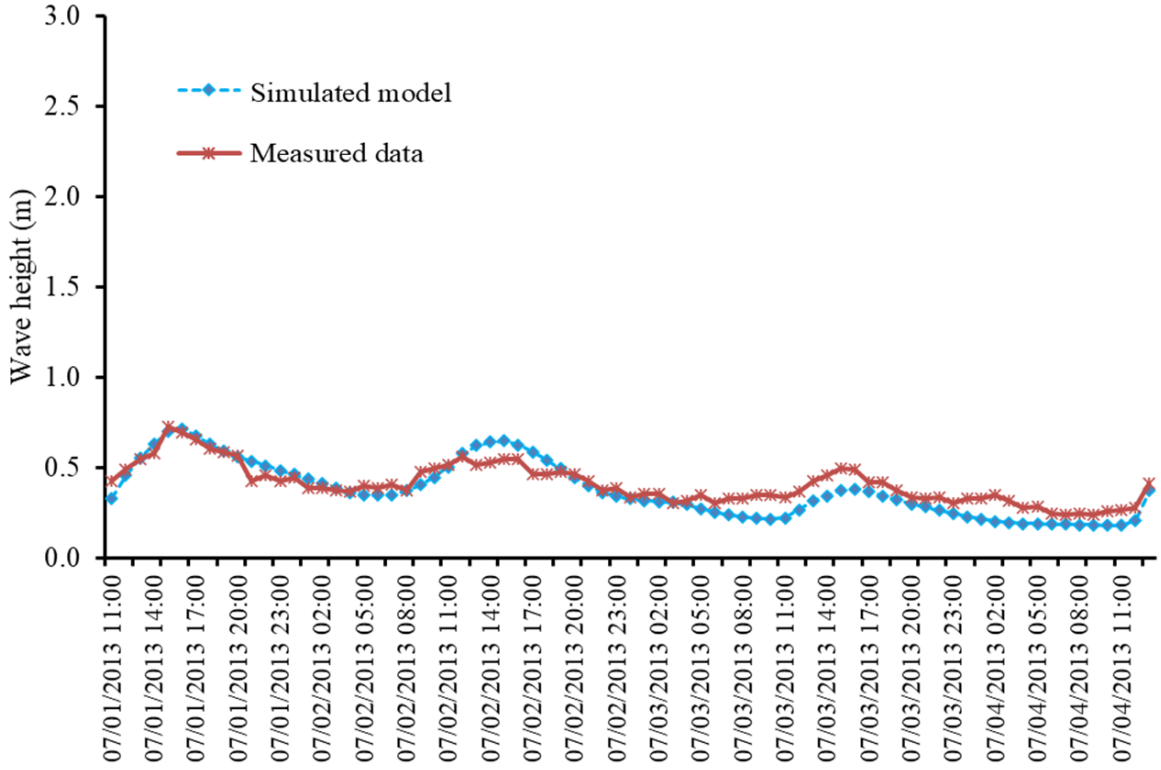

Figure 7. Comparison of the simulated model and measured data wave height during the stage from 06 to 12-Jan-2013 (Southwest monsoon) with R^2 = 0.82 and NASH = 0.75.

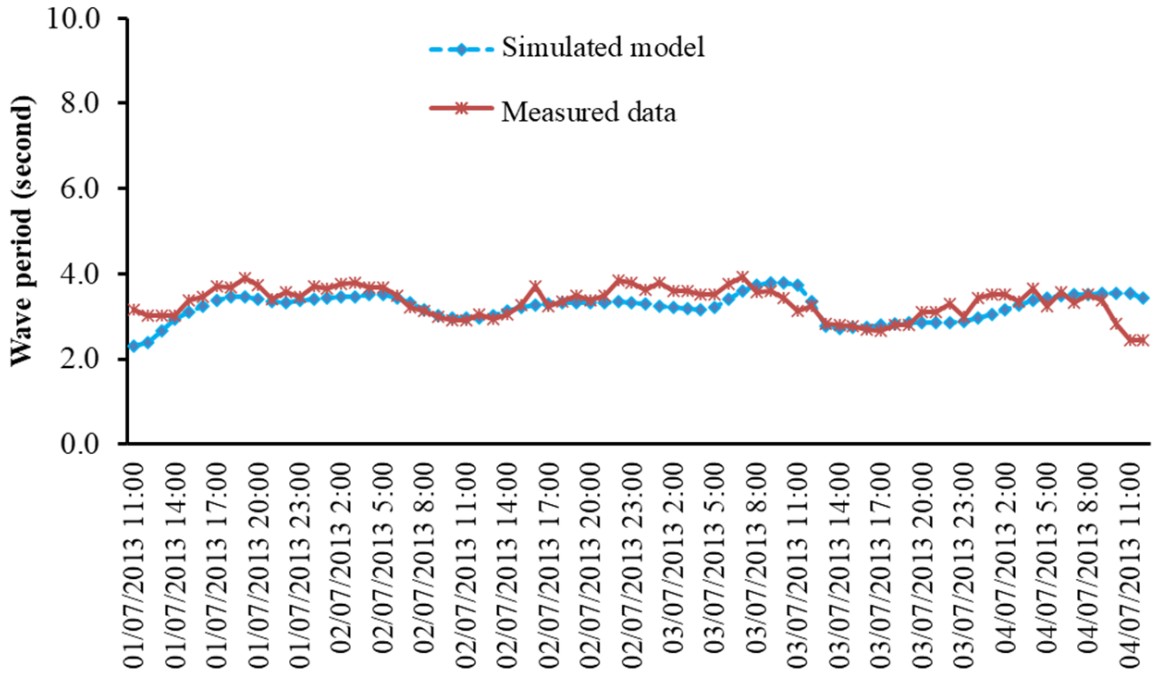

Figure 8. Comparison of the simulated model and measured data wave period during the stage from 06 to 12-Jan-2013(Southwest monsoon).

3.2. Simulation Results of the Spatial and Temporal Evolution of Rip Currents Across the Study Area

To examine the variation of rip currents according to tides, the model simulated rip currents at Bai Dai during the Northeast monsoon season under tidal fluctuations in the study area. The results of the assessment of the impact of tides on rip currents were shown at the high and low tide slopes to clearly demonstrate the impact of tidal currents on the intensity and microstructure of rip currents at Bai Dai Beach zone. The results of calculating the rip current evolution between high and low tides are shown in 3 areas as illustrated from **Figures 10** to **15**. At area I (**Figure 9**): This area has the presence of two rip currents, the positions of these two rip currents are the same between high tide and low tide phases. In terms of magnitude, when the tide height is low, the rip current speed is larger than that of the high tide phase, about 0.1–0.2 m s^{-1}. For the rip current in the North of area I, the head of the rip current extends out to the sea and the rip current speed is significantly larger than that of the high tide phase, which proves that there is a resonance of the tidal flow into the intensity of the rip current and this is one of the reasons why it is more dangerous for beachgoers than the high tide phase.

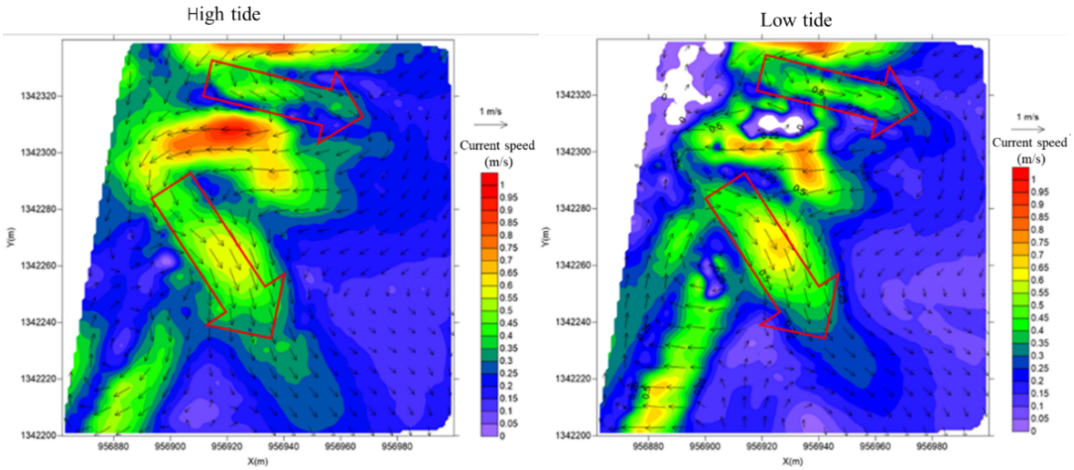

Figure 9. Simulation results of rip current at Bai Dai Beach (area I) during high tide and low tide phases in the Northeast monsoon season.

In area II (**Figure 10**): This area has the presence of two rip currents with the rip current speed greater when the tide is low, specifically, at the beginning of the rip current at high tide phase, the rip current speed is approximately 0.3 m s^{-1}, but at the same location at low tide phase the rip current speed is up to 0.5 m s^{-1}, the width of the rip current is narrower by about 2–5 m and longer than the rip current at high tide phase around 5–10 m.

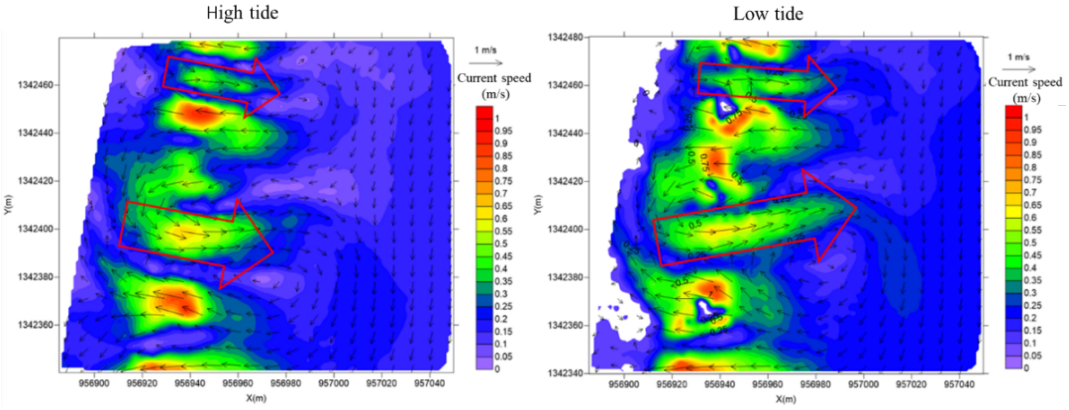

Figure 10. Simulation results of rip current at Bai Dai Beach (area II) during high tide and low tide phases in the Northeast monsoon season.

In area III (**Figure 11**): Area III records two rip currents; at low tide phase, these are two rip currents that are quite long and the rip current speed is about 2 times larger than at high tide phase. At the same time, both rip currents are directed straight towards the sea. When the tide recedes, both rip currents are wider and longer than the high tide phase and the rip current reaches a large value along the entire length of the rip current. In general, when the tide rises, the danger level of these two rip currents for swimmers is only at an average level, but when the tide recedes, the danger level of the rip currents for swimmers reaches a high-risk level.

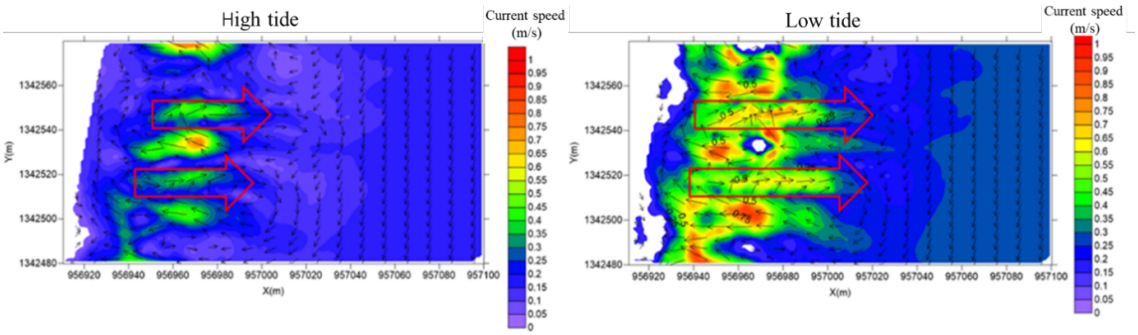

Figure 11. Simulation results of rip current at Bai Dai Beach (area III) during high tide and low tide phases in the Northeast monsoon season.

In area IV (**Figure 12**): The simulation results show that 2 rip currents appear; their locations are the same when the tide is high and low. In terms of rip current velocity and microscopic (width and length) of the rip current, there are similar differences as in area III. When the tide is high, the danger level of these 2 rip currents is only at an average level, but when the tide is low, the danger level of the rip current for swimmers is assessed as high.

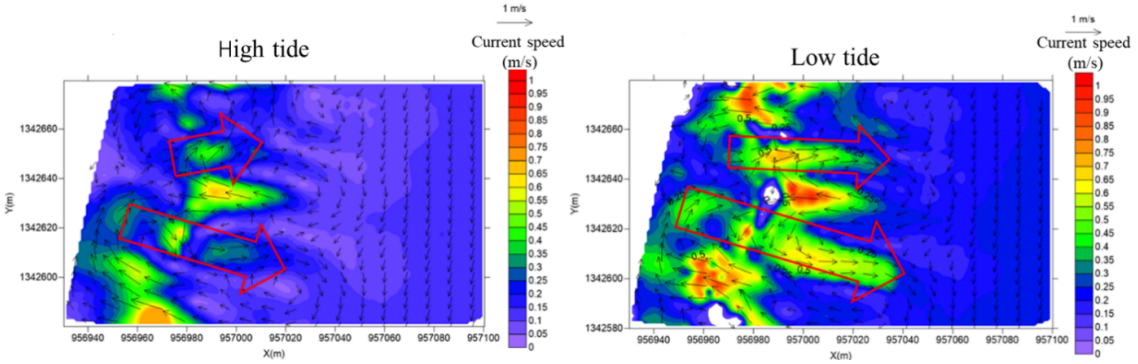

Figure 12. Simulation results of rip current at Bai Dai Beach (area IV) during high tide and low tide phases in the Northeast monsoon season.

In area V (**Figure 13**): In this area, a rip current appears with the position of the rip current's foot differing between the rising tide and the ebb tide. When the tide recedes, the rip current's foot moves about 5.0 m seaward compared to the rising tide. The rip current's velocity at ebb tide is about 0.8 m s^{-1}. This implies that there are potential risks for swimmers. Meanwhile, during the rising tide, the rip current's velocity is only about 0.4 m s^{-1} (the risk of drowning for swimmers is moderate). In terms of the width and length of the rip current, during low tide, the rip current is about 5.0–7.0 m wider than during the rising tide and the recorded length of the rip current is about 5.0–8.0 m longer than during the rising tide.

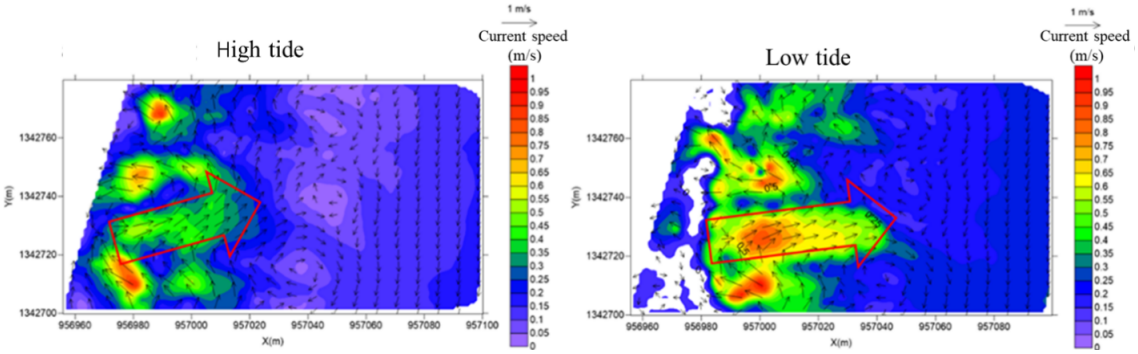

Figure 13. Simulation results of rip current at Bai Dai Beach (area V) during high tide and low tide phases in the Northeast monsoon season.

In area VI (**Figure 14**): In this area, 3 rip currents appear; the difference in shape and size of these 3 rip currents between the high and low tide phases is similar to that of area V. Regarding the location of appearance, at low tide, the position of the rip current foot is shifted out to sea about 4.0–8.0 m, the width and length of the rip current are also larger than at high tide. Regarding the rip current velocity, at low tide, the rip current has a velocity of about 0.6–0.7 m s^{-1} while at high tide, the rip current velocity is only about 0.4–0.5 m s^{-1}.

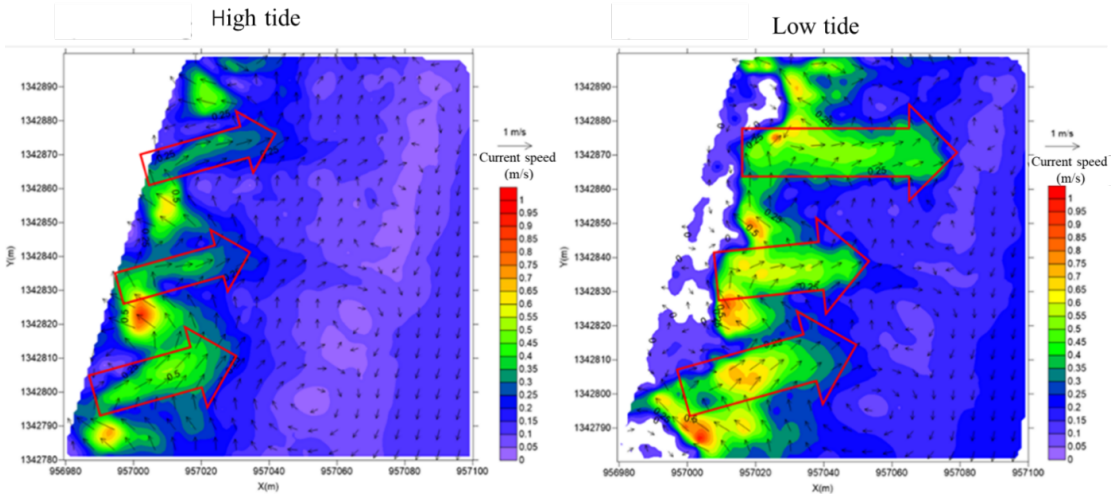

Figure 14. Simulation results of rip current at Bai Dai Beach (area VI) during high tide and low tide phases in the Northeast monsoon season.

4. Conclusions

The present study is conducted to develop a two-dimensional hydrodynamic model simulating rip currents in the Bai Dai-Cam Ranh coast of Khanh Hoa Province, Vietnam. The HYDIST-2D numerical model was applied to simulate the rip current evolution in space and time for the study area. The results showed that the model can accurately predict the location, magnitude, and microstructure of rip currents, including rip current speed, width and length.

The simulation results revealed that the rip current speed is greater during the low tide phase, with an average speed of 0.1–0.2 m s^{-1}, while during high tide, the rip current speed is lower, around 0.05–0.1 m s^{-1}. The width and length of the rip current also vary with the tide phase, with a wider and longer rip current observed during the low tide phase. The results also showed that the rip current speed and microstructure are influenced by the bathymetry of the study area.

The present study provides valuable insights into the dynamics of rip currents in the Bai Dai-Cam Ranh coast and can be used to support the management of bathing activities and provide early warnings for potential risks associated with rip currents. The model can also be applied to other

coastal areas with similar hydrodynamic conditions, making it a useful tool for coastal zone management and planning.

The findings of this study contribute to the existing literature on rip currents and their impact on drowning risks. The study highlights the importance of considering the hydrodynamic conditions of the study area when developing models to simulate rip currents. The results also demonstrate the potential of the HYDIST-2D model in predicting rip current evolution and can be used as a basis for further research on this topic.

Future studies should aim to improve the model by incorporating three-dimensional hydrodynamic processes and applying it to other coastal areas with different hydrodynamic conditions.

In conclusion, the present study demonstrates the potential of the HYDIST-2D model in simulating rip currents in the Bai Dai-Cam Ranh coast of Khanh Hoa Province, Vietnam. The results provide valuable insights into the dynamics of rip currents and can be used to support the management of bathing activities and provide early warnings for potential risks associated with rip currents. The study contributes to the existing literature on rip currents and their impact on coastal erosion and drowning risks and highlights the importance of considering the hydrodynamic conditions of the study area when developing models to simulate rip currents.

Author Contributions

Conceptualization, N.N.T. and N.T.B.; data curation: N.N.T. and N.T.B.; writing—original draft preparation, N.N.T.; writing—review and editing, N.N.T. and N.T.B. All authors have read and agreed to the published version of the manuscript.

Funding

This research did not receive any funding.

Institutional Review Board Statement

Not applicable.

Informed Consent Statement

Not applicable.

Data Availability Statement

The data supporting the findings of this study have been generated but are not currently available in a public repository. The data can be made available by the corresponding author upon reasonable request.

Acknowledgments

The authors would like to sincerely thank Dr. Le Dinh Mau, Institute of Oceanography-Vietnam Academy of Science and Technology for providing measurement data on topography, waves and currents in the research area. In addition, we would like to thank Dr. Tran Thi Kim, University of Natural Resources and Environment, Ho Chi Minh City and MSc Tra Nguyen Quynh Nga, University of Technology, Vietnam National University, Ho Chi Minh City for allowing us to continue developing the wave scattering stress calculation module.

Conflicts of Interest

The authors declare that this manuscript represents original work that has not been published previously and is not under consideration for publication elsewhere. The research was conducted by the author team without any plagiarism from previous studies. There are no conflicts of interest among the authors.

References

[1] Castelle, B., Scott, T., Brander, R.W., et al., 2016. Rip Current Types, Circulation, and Hazard. Earth Science Reviews. 163, 1–21. DOI: https://doi.org/10.1016/j.earscirev.2016.09.008

[2] Brander, R., Scott, T., 2016. Science of the rip current hazard. In: Tipton, M., Wooler, A. (eds.). The Science of Beach Lifeguarding. CRC Press: Boca Raton, FL, USA. pp. 67–86. DOI: https://doi.org/10.4324/9781315371641

[3] Dalrymple, R.A., MacMahan, J.H., Reniers, A.J.H.M., et al., 2011. Rip Currents. Annual Review of Fluid Mechanics. 43, 551–581. DOI: https://doi.org/10.1146/annurev-fluid-122109-160733

[4] Wang, Y., Zou, Z., Liu, Z., 2024. Vertical distribution of rip currents generated by intersecting waves in a sandbar—groin systems. Journal of Marine Science and Engineering. 12, 911. DOI: https://doi.org/10.3390/jm

se12060911

[5] Xu, J., Yan, S., Zou, Z., et al., 2023. Flow characteristics of the rip current system near a shore-normal structure with regular waves. Journal of Marine Science and Engineering. 11, 1297. DOI: https://doi.org/10.3390/jmse11071297

[6] Scott, T., Austin, M., Masselink, G., et al., 2016. Dynamics of rip currents associated with groynes – field measurements, modelling and implications for beach safety. Coastal Engineering. 107, 53–69. DOI: https://doi.org/10.1016/j.coastaleng.2015.09.013

[7] Da Silva, R.F., Hansen, J.E., Rijnsdorp, D.P., et al., 2022. The influence of submerged coastal structures on nearshore flows and wave runup. Coastal Engineering. 177, 104194. DOI: https://doi.org/10.1016/j.coastaleng.2022.104194

[8] Gensini, V.A., Ashley, W.S., 2010. Reply to "rip current misunderstandings". Natural Hazards. 55, 163–165. DOI: https://doi.org/10.1007/s11069-010-9528-3

[9] López-Ramade, E., Mulligan, R.P., Medellín, G., et al., 2023. Modelling beach morphological responses near coastal structures under oblique waves driven by sea-breezes. Coastal Engineering. 182, 104290. DOI: https://doi.org/10.1016/j.coastaleng.2023.10429

[10] Fang, K.Z., Yin, J.W., Zou, Z.L., et al., 2014. Reproducing laboratory-scale rip currents on a barred beach by a boussinesq wave model. Journal of Marine Science and Technology. 22, 231–239. DOI: https://doi.org/10.6119/JMST-013-0509-1

[11] Hur, D.S., Lee, W.D., Cho, W.C., et al., 2019. Rip current reduction at the open inlet between double submerged breakwaters by installing a drainage channel. Ocean Engineering. 193, 106580. DOI: https://doi.org/10.1016/j.oceaneng.2019.106580

[12] Brighton, B., Sherker, S., Brander, R., et al., 2013. Rip current related drowning deaths and rescues in Australia 2004–2011. Natural Hazards, and Earth System Sciences. 13, 1069–1075. DOI: https://doi.org/10.5194/nhess-13-1069-2013

[13] Alkan, S., Karadurmuş, U., 2023. Risk assessment of natural and other hazard factors on drowning incidents in Turkey. Natural Hazards. 118, 2459–2475. DOI: https://doi.org/10.1007/s11069-023-06095-7

[14] Moulton, M., Dusek, G., Elgar, S., et al., 2017. Comparison of rip current hazard likelihood forecasts with observed rip current speeds. American Meteorological Society. 32, 1659–1666. DOI: https://doi.org/10.1175/WAF-D-17-0076.1

[15] Ngo, N.T., Nguyen, T.B., 2023. Applicability of the MIKE21 model for simulating the rip current: A case study for Cam Ranh bay, Khanh Hoa coastal of Vietnam. Physical Oceanography. 30, 508–521.

[16] Kim, H.D., Kim, K.H., 2021. Analysis of Rip Current Characteristics Using Dye Tracking Method. Atmosphere, 12, 719. DOI: https://doi.org/10.3390/atmos12060719

[17] Klonaris, G.T., Metallinos, A.S., Memos, C.D., et al., 2020. Experimental and numerical investigation of bed morphology in the lee of porous submerged breakwaters. Coastal Engineering. 155, 103591. DOI: https://doi.org/10.1016/j.coastaleng.2019.103591

[18] Haller, M.C., Dalrymple, R.A., Svendsen, I.A., 1997. Rip channels and nearshore circulation. Proceedings of the International Conference on Coastal Research through Large Scale Experiments; June 23–27, 1997; Plymouth, UK; pp. 594–603.

[19] Li, Z., 2016. Rip current hazards in South China headland beaches. Ocean & Coastal Management. 121, 23–32. DOI: https://doi.org/10.1016/j.ocecoaman.2015.12.005

[20] McCarroll, R.J., Brander, R.W., MacMahan, J.H., et al., 2013. Assessing the effectiveness of rip current swimmer escape strategies, Shelly Beach, NSW, Australia. Journal of Coastal Research. 65, 784–789.

[21] Mucerino, L., Carpi, L., Schiafno, C.F., et al., 2021. Correction to: Rip current hazard assessment on a sandy beach in Liguria, NW Mediterranean. Natural Hazards. 105, 137–156. DOI: https://doi.org/10.1007/s11069-020-04299-9

[22] Kennedy, A.B., Zhang, Y., Haas, K.A., 2008. Rip currents with varying gap widths. Journal of Waterway Port, Coastal, and Ocean Engineering. 134, 61–65. DOI: https://doi.org/10.1061/(ASCE)0733-950X(2008)134:1(61)

[23] Drønen, N., Karunarathna, H., Fredsøe, J., et al., 2002. An experimental study of rip channel flow. Coastal Engineering. 45, 223–238. DOI: https://doi.org/10.1016/S0378-3839(02)00035-2

[24] Hu, P., Li, Z., Zhu, D., et al., 2022. Field observation and numerical analysis of rip currents at Ten-Mile Beach, Hailing Island, China. Estuarine, Coastal and Shelf Science, 276, 108014. DOI: https://doi.org/10.1016/j.ecss.2022.108014

[25] Murray, T., Cartwright, N., Tomlinson, R., 2013. Video-imaging of transient rip currents on the gold coast open beaches. Journal of Coastal Research. 65, 1809–1814.

[26] Hong, X., Zhang, Y., Wang, B., et al., 2021. Numerical study of rip currents interlaced with multichannel sandbars. Natural Hazards. 108, 593–605. DOI: https://doi.org/10.1007/s11069-021-04696-8

[27] Xu, J., Wang, Y., Mu, B., et al., 2024. Modeling rip current systems around multiple submerged breakwaters. Journal of Marine Science and Engineering. 12, 1627. DOI: https://doi.org/10.3390/jmse12091627

[28] Wang, H., Zhu, S., Li, X., et al., 2018. Numerical simulations of rip currents off arc-shaped coastlines. Acta Oceanologica Sinica. 37, 21–30. DOI: https://doi.org/10.1007/s13131-018-1197-1

[29] Nguyen, K.P., Ngo, N.T., Tran, T.H., 2012. Researching rip currents in Nha Trang Area. Advances in Science

and Technology of Water Resources. 12, 85–90.

[30] Nguyen, X.L., Dang, D.D., 2019. Assessing the possibility of appearing RIP current at Quy Nhon Beach, Binh Dinh Province. VNU Journal of Science: Earth and Environmental Sciences. 35, 34–47 DOI: https://doi.org/10.25073/2588-1094/vnuees.4416

[31] Cong, N.C., Mau, L.D., Tuan, N.V., et al., 2019. Rip current simulation on some beaches in coastal Quang Nam province. Vietnam Journal of Marine Science and Technology. 19, 113–124. DOI: https://doi.org/10.15625/1859-3097/19/3B/14519

[32] Bay, N.T., Phung, N.K., 2007. Study on the tendency of accretion and erosion in the Can Gio coastal zone. Vietnam Journal of Marine Science and Technology. 7, 50–63. DOI: https://doi.org/10.15625/1859-3097/7/4/6354

[33] Tran, T.K., Tra, N.Q.N., Nguyen, T.B., 2018. Research on the construction of a module to calculate wave scattering stress to calculate the occurrence of rip currents in coastal areas. Journal of Science and Technology. 7, 33–37.

[34] Longuet-Higgins, M.S., Stewart, R.W., 1964. Radiation stress in water waves: A physical discussion with applications. Deep Sea Research. 11, 529–563. DOI: https://doi.org/10.1016/0011-7471(64)90001-4